

Feedback control of trapped coherent atomic ensembles

T. Vanderbruggen^{1,*}, R. Kohlhaas¹, A. Bertoldi^{1,3}, S. Bernon^{1,†}, A. Aspect¹, A. Landragin², and P. Bouyer^{1,3}

¹*Laboratoire Charles Fabry, Institut d'Optique, CNRS, Université Paris-Sud*

Campus Polytechnique, RD 128, 91127 Palaiseau, France

²*LNE-SYRTE, Observatoire de Paris, CNRS and UPMC*

61 avenue de l'Observatoire, F-75014 Paris, France

³*Laboratoire Photonique, Numérique et Nanosciences - LP2N Université Bordeaux - IOGS - CNRS: UMR 5298*

Bât. A30, 351 cours de la liberation, Talence, France

(Dated: November 27, 2024)

We demonstrate how to use feedback to control the internal states of trapped coherent ensembles of two-level atoms, and to protect a superposition state against the decoherence induced by a collective noise. Our feedback scheme is based on weak optical measurements with negligible back-action and coherent microwave manipulations. The efficiency of the feedback system is studied for a simple binary noise model and characterized in terms of the trade-off between information retrieval and destructivity from the optical probe. We also demonstrate the correction of more general types of collective noise. This technique can be used for the operation of atomic interferometers beyond the standard Ramsey scheme, opening the way towards improved atomic sensors.

PACS numbers: 03.67.-a, 03.65.Yz, 37.30.+i

Coherent ensembles of two-level atoms, whose quantum evolution provides a fundamental oscillatory signal, are the core of many instruments based on Ramsey interferometry, like atomic clocks, magnetic field sensors, or inertial and gravitational sensors [1–3]. Trapping such atomic ensembles gives access to long observation times, and thus extreme precision, provided that one can fight the loss of coherence induced by ambient noise. A noise homogeneous over the size of the ensemble affects all the atoms in the same way. If the number of atoms is large, it becomes possible to measure the effect of this collective noise with negligible perturbation of the state of the individual systems. This can be done using weak measurements, as proposed in [4], and used for example to determine the collective atomic state of a coherent ensemble of atoms [5]. It is then possible to react on the atoms to compensate for the effect of the noise, and thus fight the corresponding decoherence. Similar techniques have been proposed to boost the performance of atomic clocks by phase-locking the local oscillator to the atomic phase [6].

In this Letter, we demonstrate such a measurement and correction scheme, using a trapped coherent ensemble of two-level atoms. The atomic system consists in rubidium 87 atoms prepared in a coherent superposition of the two ground hyperfine levels $|0\rangle \equiv |F=1, m_F=0\rangle$ and $|1\rangle \equiv |F=2, m_F=0\rangle$ of the electronic ground state $5^2S_{1/2}$. This superposition can be manipulated by the interaction with a microwave field resonant with the 6.835 GHz transition between the two levels. The population difference is weakly measured using a frequency modulated optical probe, where the sidebands are phase shifted with opposite signs by the two atomic populations. This probe is used to evaluate the effect of a collective noise on the atoms for later correction. We consider two different noise models: the first model takes randomly one of two known values, and the second one takes a random value uniformly distributed.

A sample of N_{at} indistinguishable two-level atoms can be represented as an ensemble of effective spins $1/2$, whose sum defines a collective spin, or Bloch vector, with observables $\mathbf{J} = (J_x, J_y, J_z)$ on the Bloch sphere [7, 8]. The observable J_z refers to the population difference between the two atomic levels, while J_x and J_y characterize the coherence between the two levels. When all the atoms are in the same pure single particle state, they form a coherent spin state (CSS) or Bloch state; the associated Bloch vector has its extremity on a Bloch sphere of radius $J = N_{\text{at}}/2$. Any collective and homogeneous interaction with the microwave results in a rotation of the Bloch vector. We restrict our study to rotations around Y : all accessible states are then represented by a vector in the $y = 0$ plane, labelled $|\theta\rangle$ from the angle θ it forms with the Z axis.

In our experiment we initially prepare the atoms in the CSS $|\theta = \pi/2\rangle$, which is the state after the first beamsplitter in a Ramsey interferometer sequence and for which $\langle J_z \rangle = 0$. Our goal is to recover that state after it is submitted to a collective noise (Fig. 1). The noise consists of random collective rotations (RCRs) implemented using microwave pulses that rotate the Bloch vector around the Y axis. The rotation angle is selected randomly according to each specific model. The RCR transforms the initial state into a statistical mixture of all the states that can be generated by the noise; as a consequence the length of the Bloch vector decreases from $J = N_{\text{at}}/2$ to a lesser value, thus decreasing the coherence of the initial state. We have implemented two noise models: first, a binary RCR, where the collective Bloch vector is submitted to rotations picked randomly among two fixed values $+\alpha$ and $-\alpha$; second, an analog RCR with a random rotation angle uniformly distributed between $-\alpha$ and $+\alpha$. The binary RCR transforms the initial CSS into a balanced statistical mixture of the states $|\pi/2 + \alpha\rangle$ and $|\pi/2 - \alpha\rangle$. The analog RCR transforms the initial

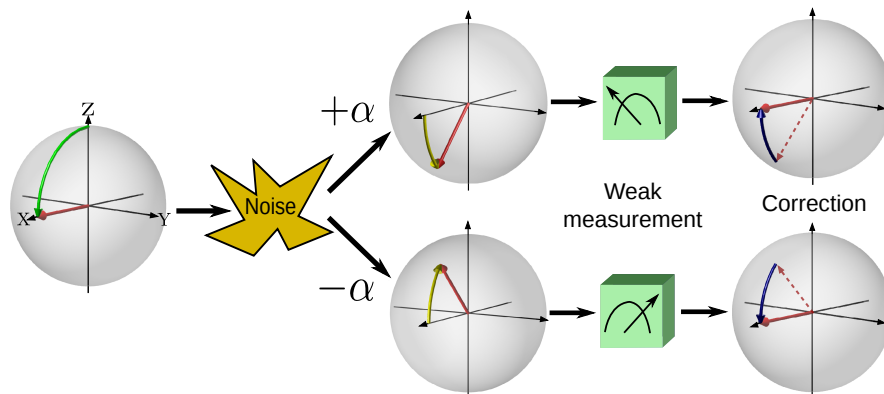


FIG. 1. (color online). Evolution of the collective spin on the Bloch sphere (case of a binary random collective rotation). A $\pi/2$ rotation around Y prepares a coherent superposition. The state experiences a random rotation of $+\alpha$ or $-\alpha$ around Y , which is detected using a weak non-destructive measurement and then corrected.

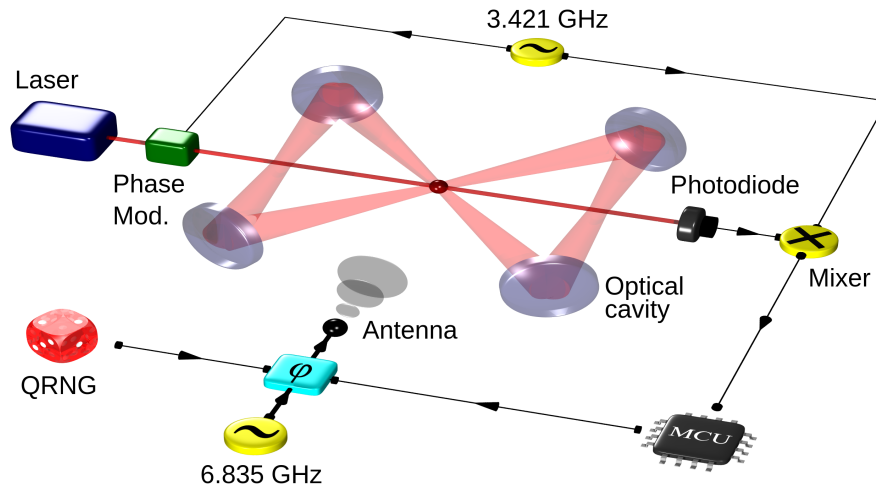


FIG. 2. (color online). Experimental setup: the atomic sample is coherently manipulated with the microwave field emitted by an antenna. The detection laser at 780 nm is phase modulated at 3.421 GHz before passing through the atomic cloud and being detected on a photodiode. After demodulation, the signal is digitized and sent to a microcontroller unit that computes and sets the phase of the microwave. A quantum random number generator (QRNG), connected to the phase-shifter (φ), implements the RCR.

CSS into the statistical mixture $\rho = 1/(2\alpha) \int_{-\alpha}^{+\alpha} |\pi/2 + \theta\rangle \langle \pi/2 + \theta| d\theta$. The coherence of the atomic ensemble then decreases from unity to $\eta_\alpha = \cos \alpha$ in the binary case, and to $\eta_\alpha = \sin \alpha / \alpha$ in the analog case.

To fight the loss of coherence induced by the noise, we optically measure J_z after each random rotation, and apply a counter-rotation depending on the result. We consider in this work only measurements with an uncertainty σ larger than the atomic projection noise ($\sigma \gg \sqrt{N_{\text{at}}}$). For large CSSs, the measurement uncertainty is small compared to the length of the spin ($\sigma < J$) and a weak measurement can lead to precise information with negligible back-action. In the binary RCR case, the probability to detect the hemisphere in which the Bloch vector lies ($z > 0$ or $z < 0$) is

$$p_s = \int_0^\infty P(m_0 | -\alpha) dm_0 = \frac{1}{2} \left[1 + \operatorname{erf} \left(\frac{\sqrt{2} J \sin \alpha}{\sigma} \right) \right], \quad (1)$$

where $P(m_0 | -\alpha)$ is the probability to obtain m_0 when measuring J_z given a noise rotation $-\alpha$. After the correction the system is in a statistical mixture of the initial state $|\pi/2\rangle$, recovered with probability p_s , and of the two states $|\pi/2 \pm 2\alpha\rangle$ resulting from a wrong estimation that doubles the RCR angle. The coherence of this statistical mixture is

$$\eta_\alpha^{\text{out}} = [p_s + (1 - p_s) \cos(2\alpha)] e^{-\gamma N_{\text{ph}}}, \quad (2)$$

where the exponential factor accounts for the effect of the spontaneous emission induced by N_{ph} photons in the probe pulse, and the coefficient γ , which depends on the resonant optical density, is determined experimentally (see below).

We work with 5×10^5 ^{87}Rb atoms at $T=10$ μK , optically trapped by laser light at 1550 nm (Fig. 2). The laser intensity is enhanced using a 4 mirror optical resonator [9]. The atomic cloud (radius at $1/e^2$ of 50 μm) is trapped where two cavity arms (waist of 100 μm) cross. The radiation that traps the atoms in $|0\rangle$ and $|1\rangle$, generates a strong, spatially inhomogeneous broadening of the D_2 transition [2], used for the probing. The effect is compensated by modifying the light shift of the $5^2\text{P}_{3/2}$ level using an auxiliary, spatially matched laser beam [11]. The non-destructive detection of J_z is based on the phase-shift that the atomic sample induces on a far off-resonance optical probe [9, 12–16]. The probe beam has a waist of 245 μm on the atomic sample. It is phase modulated at a frequency $\Omega = 3.421$ GHz, and frequency referenced so that each sideband mainly probes the population of one of the two levels $|0\rangle$ and $|1\rangle$, with the same magnitude and opposite sign for the couplings [11, 17]. We cancel the probe induced light shift and the related decoherence by precisely compensating the effect of the carrier with that of the sidebands [11].

We prepare the initial CSS $|\theta = \pi/2\rangle$ by optically pumping the atoms in $|0\rangle$ and applying a $\pi/2$ microwave pulse of duration $\tau_{\pi/2} = 75.6(2)$ μs . We study the control process consisting of a binary RCR, a weak measurement pulse to determine the sign of J_z , and a correcting rotation. The binary RCR is implemented as a $\alpha = \pi/4$ microwave pulse; the coherence after the noise and after the correction is $\eta_{\pi/4} = 1/\sqrt{2}$ and $\eta_{\pi/4}^{\text{out}} = p_s e^{-\gamma N_{\text{ph}}}$ (see Eq. (2)), respectively.

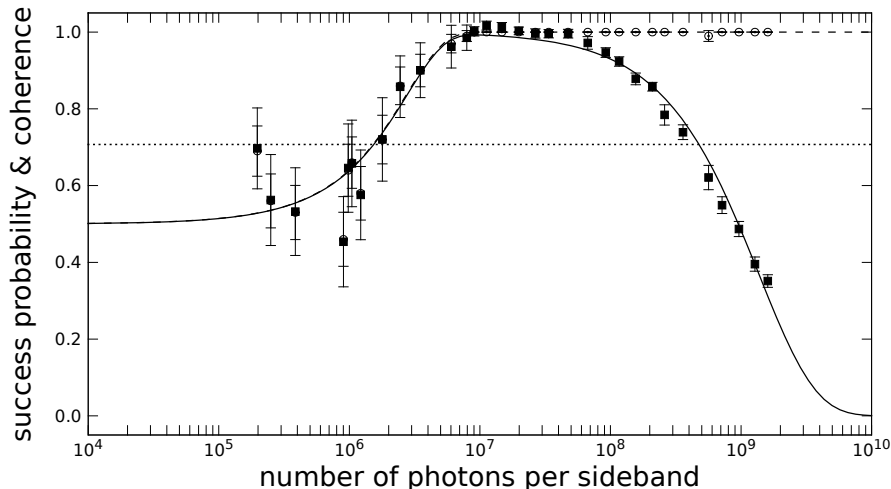


FIG. 3. Remaining coherence (solid squares) after the cycle consisting of a binary RCR, measurement and correction; success probability (open circles) versus the number of photons per sideband in the probe pulse. The solid line is a fit of the remaining coherence data with Eq. (2), the dashed one of the success probability data with Eq. (1). The dotted line at $1/\sqrt{2}$ indicates the coherence after the RCR. Error bars are the ± 1 standard error of statistical fluctuations.

The spontaneous emission due to the carrier is negligible compared to that of the sidebands, hence N_{ph} relates to the number of photons in each sideband. The rotation sign is randomly chosen by a quantum random number generator (Quantis, IDQuantique) and set through a phase-shifter on the microwave. The J_z measurement uses a $1.5 \mu\text{s}$ long probe pulse. The detected signal is demodulated to get the population difference, and then analogically integrated to obtain its mean value over the pulse length. To implement the feedback, the output of the integrator is digitized and treated in real-time with a microcontroller to get the sign of J_z . The latter controls the rotation direction for the $\pi/4$ correction pulse through the microwave phase-shifter.

We evaluate the efficiency of the feedback control in terms of the achieved coherence recovery. To determine the coherence of the atomic state at the end of the cycle, we send a second $\pi/2$ pulse to obtain a Ramsey type measurement. Fig. 3 shows the remaining coherence after one cycle (solid squares), when the measurement uncertainty σ is varied by changing the number of photons in the probe pulse. Each point results from 50 repetitions of the sequence, and the reported error bars reflect the statistical spread. We fitted the data set with Eq. (2) for $\eta_{\pi/4}^{\text{out}}$, using Eq. (1) for the success probability p_s and assuming for σ two contributions, one related to the photonic shot noise ($\propto N_{\text{ph}}^{-1/2}$) and one to technical noise ($\propto N_{\text{ph}}^{-1}$): the latter is dominant and we obtain $\sigma = 9.6(5) \times 10^{11}/N_{\text{ph}}$ [18]. The fit of Fig. 3 yields also the rate for the probe induced decoherence per photon $\gamma = 7.6(4) \times 10^{-10}$. The remaining coherence of the output state reaches an optimum of $0.993(1)$ with 9.1×10^6 photons per sideband: this value exceeds the coherence $1/\sqrt{2} \approx 0.707$ of the mixed state after the RCR, proving the efficiency of our scheme.

We confirmed this result by multiplying the success probability p_s of detecting the right hemisphere and the probe induced decoherence measured separately using Ramsey interferometry. To obtain p_s , the sign of the RCR and the corresponding correction are recorded during the experiment; treated off-line they produce the open circles of Fig. 3, fitted with Eq. (1).

To study how the feedback scheme can protect a CSS over time in the presence of noise, we iterate 200 times on the same atomic ensemble the cycle consisting of the binary RCR of angle $\pi/4$, the weak measurement of J_z , and the corresponding correction rotation. At each cycle J_z is measured by integrating the signal determined by 1.4×10^7 photons in each sideband.

During that experiment the signs of the RCRs and the corresponding corrections are recorded; analyzed off-line they provide the trajectory followed by the Bloch vector. The state occupancy, which is the probability to be in a given state, is measured versus time averaging the results of 200 experimental runs. In the closed loop case, the system spreads from $|\pi/2\rangle$ to the two poles ($|0\rangle, |\pi\rangle$), and at a slower rate to $|3\pi/2\rangle$ (Fig. 4(a), points). The evolution of the state occupancy over the four states is explained in terms of the random rotations of $\pm\pi/4$ at every cycle, and by the success probability p_s of the weak measurement (Fig. 4(a), solid lines). At each cycle, p_s decreases since the spontaneous emission induced by the probe and the residual inhomogeneous differential light shift of the trap shorten the spin. The trap induced decoherence has been characterized by Ramsey interferometry, and the coherence loss

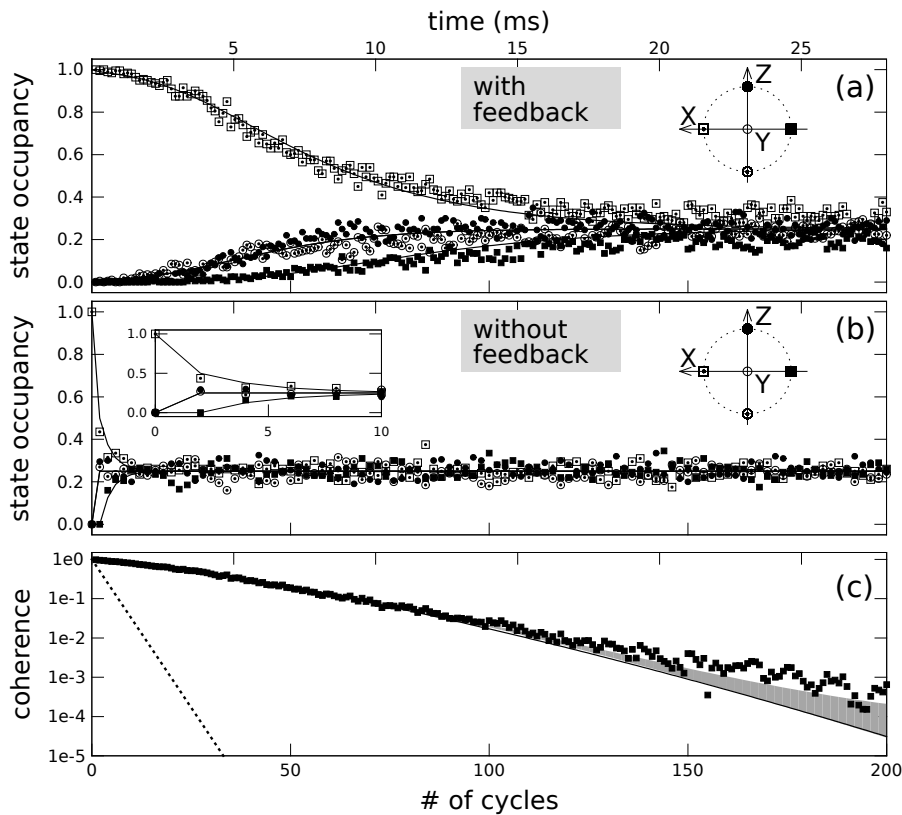


FIG. 4. State occupancy versus the number of cycles for the state $|0\rangle$ (solid circles), $|\pi/2\rangle$ (open squares), $|\pi\rangle$ (open circles) and $|3\pi/2\rangle$ (solid squares) with (a) and without (b) feedback correction. Each experimental point is obtained from 200 repetitions of the sequence. One cycle lasts $140 \mu\text{s}$. The solid lines are calculated independently, considering the probabilistic outcome of the RCRs, and in closed-loop that of the corresponding corrections. Inset: In the open loop case, the state occupancy is equally distributed over the four states after about 10 cycles. (c) Calculated remaining coherence with (solid line) and without (dashed line) feedback. The experimental points in closed-loop are shifted at the top of the shaded region because of the finite size statistical sample in the state occupancy determination.

versus the time in the dipole trap shows a Gaussian decay. Considering the cycle duration, the trap decoherence can be expressed in terms of the number of cycles N as $\exp(-(N/N_0)^2)$, where $N_0 = 157.6$. This decoherence is not a limitation in the present case and could be further reduced using a compensation laser beam [19, 20].

The state occupancy is compared to the open-loop case, where measurements and corrections are not applied: after a few iterations the state vector reaches a balanced statistical mixture of four states: $\{|0\rangle, |\pi/2\rangle, |\pi\rangle, |3\pi/2\rangle\}$ for an even number of iterations, and $\{|\pi/4\rangle, |3\pi/4\rangle, |5\pi/4\rangle, |7\pi/4\rangle\}$ for an odd number (Fig. 4(b), points). Here the state occupancy evolution results only from the random rotations of $\pm\pi/4$ at every cycle (Fig. 4(b), solid lines).

The remaining coherence has been evaluated by multiplying the effects of the decoherence sources (Fig. 4(c)), while the spin rotations are considered perfect. In open-loop the remaining coherence given by the spin diffusion, equal to $\eta_{\pi/4}^N = 1/2^{N/2}$, has to be multiplied by the effect of the trap. In closed-loop the factors to consider to obtain the coherence reduction are given by the state occupancy evolution, the probe spontaneous emission, and the trap. The feedback correction greatly improves the coherence lifetime of the system even when the experimental imperfections and limitations are taken into account: for example, after $N = 10$ cycles the remaining coherence without feedback is 0.03 whereas it reaches 0.77 when a correction is applied.

We now study the case of an analog RCR with a random rotation angle uniformly distributed on $[-\pi/2, +\pi/2]$ and acting on $|\pi/2\rangle$; this generates a statistical mixture with coherence $\eta_{\pi/2} = 2/\pi$. The analog RCR is implemented using the quantum random number generator to control both the length of the microwave pulse and the rotation sign. After the RCR, a probe pulse with 2.8×10^7 photons is sent to measure J_z . From the measurement result, we set both the length and the direction of the correction pulse. The feedback bandwidth is about 10 kHz and is limited by the duration of the correction pulse, which is set as a function of the measured value of J_z .

As reported for the binary RCR case, the coherence of the state after one cycle with and without feedback is directly

measured by Ramsey interferometry. Averaging over 400 repetitions, the coherence obtained without feedback is $0.63(3)$, consistent with the expected value of $2/\pi \approx 0.637$; the correction pulse increases the coherence to $0.964(5)$.

We can again compare the measured value of the coherence after one cycle to the value obtained by multiplying the effects of the different decoherence sources. To evaluate the decoherence due to the direction spread of the spin, during each sequence we record the length τ_N and the direction ϵ_N (+/-1 for a pos./neg. rotation) for the noise pulse, and the corresponding parameters τ_C and ϵ_C for the correction pulse. The spin direction is then computed as $\theta_N = \pi\epsilon_N(\tau_N/\tau_\pi)$ for the CSS after the noise pulse, $\theta_C = \theta_N + \pi\epsilon_C(\tau_C/\tau_\pi)$ after the correction pulse. For 5000 repetitions of the sequence θ_N is uniformly distributed over $[-\pi/2, +\pi/2]$ whereas θ_C is well described by a Gaussian distribution centered at zero and of standard deviation $207(10)$ mrad. The angular spread is explained in terms of the measurement uncertainty of 6.8% over J_z , increased by a factor 2 because of a resolution loss in the digital controller. The remaining coherence for the spin spread is $0.979(2)$. The probe induced spontaneous emission reduces the coherence by another factor $0.979(1)$. The product of these two factors gives a final remaining coherence of $0.958(2)$, which is consistent with its direct measurement.

To summarize, we have demonstrated the partial protection of an atomic CSS from the decoherence induced by RCRs around a fixed axis, using feedback control based on weak non-destructive measurements. The method can be generalized to rotations around an arbitrary axis of the Bloch sphere: one could consecutively read out J_x , J_y and J_z and correct with suitable rotations. Compared to spin-echo techniques, relying on temporal invariance of the noise, our feedback method allows the compensation of time dependent noise, provided that the time evolution is slower than the correction time. By increasing the effective on-resonance optical depth, the feedback scheme could be implemented in the projective limit to deterministically prepare non-classical states [21–23], using measurement based spin squeezing [12, 13, 24, 25]. Finally, we note that coherence preserving techniques that combine repeated measurements and feedback pave the way towards novel atom interferometry schemes, as recently proposed with atomic clocks to achieve white phase noise [6].

We thank A. Browaeys for comments. We acknowledge funding from DGA, IFRAF, CNES, the European Union (EU) (iSENSE), EURAMET (QESOCAS), ANR (MINIATOM), and ESF Euroquam. A. A. acknowledges support from ERC QUANTATOP, P. B. from a chair of excellence of Région Aquitaine.

* Now at: ICFO - Institut de Ciències Fotòniques, E-08860 Castelldefels (Barcelona), Spain

† Now at: Universität Tübingen, D-72076 Tübingen, Germany

- [1] A. D. Cronin, J. Schmiedmayer, and D. E. Pritchard, *Rev. Mod. Phys.* **81**, 1051 (2009).
- [2] D. Budker and M. Romalis, *Nat. Phys.* **3**, 227 (2007).
- [3] J. Guéna, M. Abgrall, D. Rovera, P. Laurent, B. Chupin, M. Lours, G. Santarelli, P. Rosenbusch, M. E. Tobar, R. Li, K. Gibble, A. Clairon and S. Bize, *IEEE T. Ultrason. Ferr.* **59**, 391 (2012).
- [4] S. Lloyd and J.-J. E. Slotine, *Phys. Rev. A* **62**, 012307 (2000).
- [5] G. A. Smith, A. Silberfarb, I. H. Deutsch, and P. S. Jessen, *Phys. Rev. Lett.* **97**, 180403 (2006).
- [6] N. Shiga and M. Takeuchi, *New J. Phys.* **14**, 023034 (2012).
- [7] F. T. Arecchi, E. Courtens, R. Gilmore, and H. Thomas, *Phys. Rev. A* **6**, 2211 (1972).
- [8] W. M. Itano, J. C. Bergquist, J. J. Bollinger, J. M. Gilligan, D. J. Heinzen, F. L. Moore, M. G. Raizen, and D. J. Wineland, *Phys. Rev. A* **47**, 3554 (1993).
- [9] S. Bernon, T. Vanderbruggen, R. Kohlhaas, A. Bertoldi, A. Landragin, and P. Bouyer, *New J. Phys.* **13**, 065021 (2011).
- [2] A. Bertoldi, S. Bernon, T. Vanderbruggen, A. Landragin, and P. Bouyer, *Opt. Lett.* **35**, 3769 (2010).
- [11] See Supplemental Material.
- [12] J. Appel, P. J. Windpassinger, D. Oblak, U. B. Hoff, N. Kjærgaard, and E. S. Polzik, *Proc. Natl. Acad. Sci. USA* **106**, 10960 (2009).
- [13] M. H. Schleier-Smith, I. D. Leroux, and V. Vuletić, *Phys. Rev. Lett.* **104**, 073604 (2010).
- [14] M. Koschorreck, M. Napolitano, B. Dubost, and M. W. Mitchell, *Phys. Rev. Lett.* **105**, 093602 (2010).
- [15] M. Kohnen, P. G. Petrov, R. A. Nyman, and E. A. Hinds, *New J. Phys.* **13**, 085006 (2011).
- [16] T. Vanderbruggen, S. Bernon, A. Bertoldi, A. Landragin, and P. Bouyer, *Phys. Rev. A* **83**, 013821 (2011).
- [17] M. Saffman, D. Oblak, J. Appel, and E. S. Polzik, *Phys. Rev. A* **79**, 023831 (2009).
- [18] A consistent uncertainty value of $\sigma = 3.4 \times 10^4$ was obtained by measuring the operator J_z on 5×10^5 atoms in the $|\pi/2\rangle$ state with $N_{\text{ph}} = 2.8 \times 10^7$. In the same conditions the width of the atomic distribution is $\sigma_{\text{at}} = 7.1 \times 10^2 \ll \sigma$, which proves the weakness of the measurement.
- [19] A. Kaplan, M. F. Andersen and N. Davidson, *Phys. Rev. A* **66**, 045401 (2002).
- [20] A. G. Radnaev, Y. O. Dudin, R. Zhao, H. H. Jen, S. D. Jenkins, A. Kuzmich and T. A. B. Kennedy, *Nature Phys.* **6**, 894 (2010).
- [21] H. M. Wiseman and G. J. Milburn, *Phys. Rev. A* **49**, 1350 (1994).
- [22] L. K. Thomsen, S. Mancini, and H. M. Wiseman, *Phys. Rev. A* **65**, 061801(R) (2002).

- [23] J. K. Stockton, J. M. Geremia, A. C. Doherty, and H. Mabuchi, Phys. Rev. A **69**, 032109 (2004).
- [24] Z. Chen, J. G. Bohnet, S. R. Sankar, J. Dai, and J. K. Thompson, Phys. Rev. Lett. **106**, 133601 (2011).
- [25] R. J. Sewell, M. Koschorreck, M. Napolitano, B. Dubost, N. Behbood, and M. W. Mitchell, Phys. Rev. Lett. **109**, 253605 (2012).

SUPPLEMENTAL MATERIAL

Measurement of the observable J_z . An optical beam is phase modulated to have 4.6% of the total power in each sideband and passes through the atomic sample before being detected on a fast photodiode. With the two sidebands generated by the phase modulator it is possible to directly measure the population difference between the hyperfine levels of the ground state for a ^{87}Rb atomic ensemble: one sideband is placed close to the $|F=1\rangle \rightarrow |F'=2\rangle$ transition, the other one close to the $|F=2\rangle \rightarrow |F'=3\rangle$ transition, as depicted in Fig. 5(b). The coupling S_1 (S_2) of the first (second) sideband with the $|F=1\rangle \rightarrow |F'=2\rangle$ ($|F=2\rangle \rightarrow |F'=3\rangle$) transition, is given by:

$$S_F = \sum_{F'} \frac{\gamma \Delta_{FF'}}{\Delta_{FF'}^2 + \gamma^2 (1 + I/I_{\text{sat}})} S_{FF'}, \quad (3)$$

where γ is the half width at half maximum of the atomic transition, I the intensity of each sideband, I_{sat} the saturation intensity of the transition and $S_{FF'}$ the dipolar coupling associated to the $|F\rangle \rightarrow |F'\rangle$ transition [1]. The phase-shift induced by the atomic sample on the probe is proportional to $\phi_{\text{at}} \propto N_1 S_1 + N_2 S_2$, where N_1 (N_2) is the population in the $|F=1\rangle$ ($|F=2\rangle$) level. If the detunings $\Delta_{FF'}$ are adjusted so that $S_1 = -S_2$, then $\phi_{\text{at}} \propto N_1 - N_2$ and the detection measures the observable J_z .

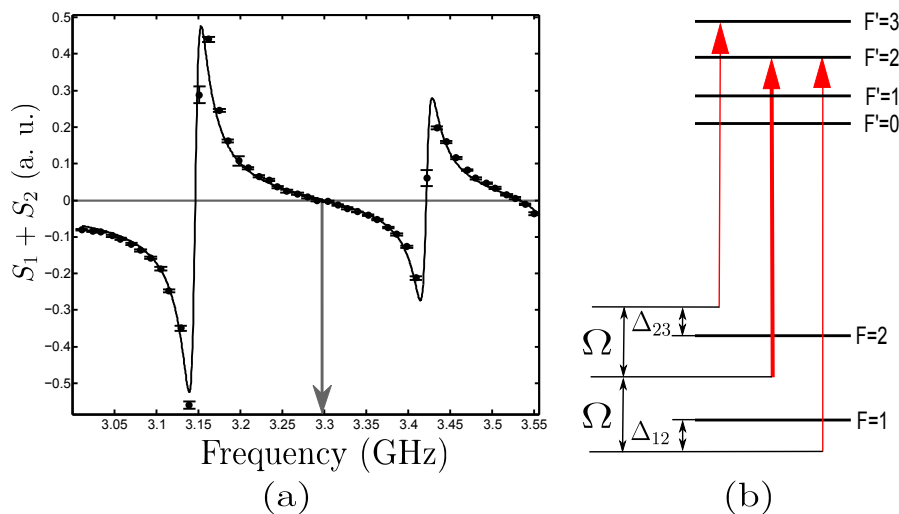


FIG. 5. (a) Coupling of the probe versus the position of the carrier with respect to the $|F=1\rangle \rightarrow |F'=2\rangle$ transition. The experimental results (filled circles) are compared to the calculated coupling (solid line). (b) Hyperfine structure of the D_2 transition of ^{87}Rb and relative position of the probing beams. The thick line is the carrier whereas the thin lines are the sidebands.

To adjust the detunings $\Delta_{FF'}$, we first set a modulation frequency $\Omega = 3.421$ GHz and prepare the atoms in a coherent superposition $|\pi/2\rangle$ so that $N_1 = N_2$. We measure then the demodulated signal versus the position of the carrier with respect to the $|F=1\rangle \rightarrow |F'=2\rangle$ transition. The result in Fig. 5(a), in very good agreement with Eq. (3), was obtained with a carrier power of $153 \mu\text{W}$ and a power per sideband of $7.1 \mu\text{W}$. The beam waist of the probe on the atomic sample is $245 \mu\text{m}$, which gives an intensity on the sample of $11.2 \text{ mW}/\text{cm}^2$. Since a π transition is probed, the saturation intensity is $I_{\text{sat}} = 2.503 \text{ mW}/\text{cm}^2$ [1]. The condition $S_1 + S_2 = 0$ is reached when the carrier is set at 3.291 GHz from the $|F=1\rangle \rightarrow |F'=2\rangle$ transition, and the detunings of the sidebands are $\Delta_{12} = -126.7$ MHz and $\Delta_{23} = 148.5$ MHz.

Compensation of the probe induced light shift. The light shift of the probe is a severe limitation in most applications using non-destructive probing techniques, especially for interferometry because it dephases the atomic sample. Here, it induces not only a rotation of the mean spin around the Z axis of the Bloch sphere but also spreads the spins due to the spatial inhomogeneity of the Gaussian probe beam. This spread acts as a decoherence source and prevents to realize the feedback scheme if not compensated. The symmetry of the coupling of each sideband with the related transition allows us to use the light shift generated by the carrier to equally compensate that of each sideband (Fig. 6(a)). Moreover, since the carrier and the sidebands are spatially overlapped the compensation is homogeneous. The compensation is realized by adjusting the relative power between the sidebands and the carrier. The tuning of the

power ratio is precisely set using a Ramsey sequence with a probe pulse sent between the two $\pi/2$ pulses. Interference fringes are scanned by changing the intensity in the sidebands (Fig. 6(b)) and the condition of maximum contrast gives the position of the zero light shift; this is obtained with 4.6% of the total power in each sideband.

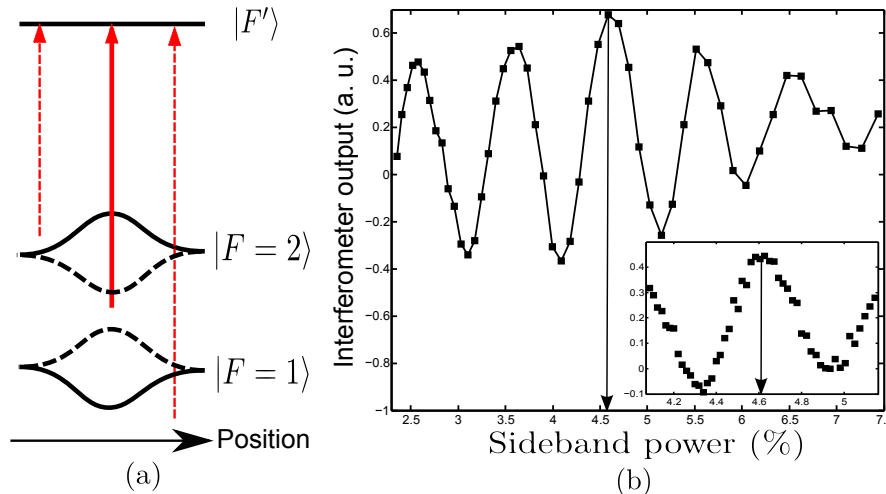


FIG. 6. (a) Light shift induced by the carrier (solid lines) and by the sidebands (dashed lines) versus the position of an atom in the probe beam. (b) Output of a Ramsey interferometer versus the power in each sideband in percent of the carrier power. A $40 \mu\text{s}$ probe pulse is sent in between the two $\pi/2$ microwave pulses. In inset, the same measurement is performed with a $70 \mu\text{s}$ long pulse to determine more precisely the compensation ratio.

Compensation of the differential light shift on the D_2 line. Due to the $5^2P_{3/2} \rightarrow 4^2D_{5/2,3/2}$ transitions at 1529.3 nm [4], the trapping radiation at 1550 nm induces a differential light shift on the D_2 transition [2] used for the non-destructive probing. At the center of the trap, where the radiation intensity is maximal, the differential frequency shift is about 100 MHz for the typical power in the optical trap: this is of the same order of Δ_{12} and Δ_{23} . In such conditions, the coupling of each atom with the probe is inhomogeneous and this hampers the measurement of the observable J_z . To compensate for the differential light shift, a radiation beam at 1528.7 nm , that is about 0.6 nm on the blue side of the $5^2P_{3/2} \rightarrow 4^2D_{5/2,3/2}$ transitions, is injected in the fundamental mode of the cavity [3]. By adjusting the power ratio between the 1550 nm and the 1529 nm beams, we compensate for the differential light shift with a high spatial homogeneity thanks to the good overlap between the fundamental modes of the cavity at 1550 nm and 1529 nm . This compensation allows for a quasi-homogeneous coupling of the non-destructive probe with the atomic sample over the spatial extension of the dipole trap. The residual light shift due to the non perfect mode overlap is about 0.7 MHz , which is not only negligible compared to Δ_{12} and Δ_{23} but also small compared to the transition linewidth ($\Gamma \sim 2\pi \cdot 6 \text{ MHz}$).

* Now at: ICFO - Institut de Ciències Fotòniques, E-08860 Castelldefels (Barcelona), Spain

† Now at: Universität Tübingen, D-72076 Tübingen, Germany

[1] D. A. Steck, *Rubidium 87 D line data* (2001).

[2] A. Bertoldi, S. Bernon, T. Vanderbruggen, A. Landragin, and P. Bouyer, *Opt. Lett.* **35**, 3769 (2010).

[3] R. Kohlhaas, T. Vanderbruggen, S. Bernon, A. Bertoldi, A. Landragin, and P. Bouyer, *Opt. Lett.* **37**, 1005 (2012).

[4] L. Lee, H. S. Moon, and H. S. Suh, *Opt. Lett.* **32**, 2810 (2007).